J Mater Sci (2010) 45:392–398
DOI 10.1007/s10853-009-3953-2

Microstructure and mechanical properties of SiC_P/SiC and SiC_W/SiC composites by CVI

Yunfeng Hua · Litong Zhang · Laifei Cheng · Zhengxian Li · Jihong Du

Received: 28 March 2009 / Accepted: 5 October 2009 / Published online: 20 October 2009

Abstract 37.2 vol.% SiC_P/SiC and 25.0 vol.% SiC_W/SiC composites were prepared by chemical vapor infiltration (CVI) process through depositing SiC matrix in the porous particulate and whisker preforms, respectively. The particulate (or whisker) preforms has two types of pores; one is small pores of several micrometers at inter-particulates (or whiskers) and the other one is large pores of hundreds micrometers at inter-agglomerates. The microstructure and mechanical properties of 37.2 vol.% SiC_P/SiC and 25.0 vol.% SiC_W/SiC composites were studied. 37.2 vol.% SiC_P/SiC (or 25.0 vol.% SiC_W/SiC) consisted of the particulate (or whisker) reinforced SiC agglomerates, SiC matrix phase located inter-agglomerates and two types of pores located inter-particulates (or whiskers) and inter-agglomerates. The density, fracture toughness evaluated by SENB method, and flexural strength of 37.2 vol.% SiC_P/SiC and 25.0 vol.% SiC_W/SiC composites were 2.94 and 2.88 g/cm^3, 6.18 and 8.34 MPa m$^{1/2}$, and 373 and 425 MPa, respectively. The main toughening mechanism was crack deflection and bridging.

Introduction

Silicon carbide (SiC) is one of the promising candidate ceramic materials for a variety of high temperature, high stress and severe erosion applications in the aerospace, hot engine, and energy conversion devices because of its excellent high temperature properties. However, its low fracture toughness (2.5–3 MPa m$^{1/2}$) has long hindered this material from being used for wide applications. One of the solutions under investigation is to increase its fracture toughness by changing the microstructure through incorporating rodlike SiC particulates or grains [1–6], growing fine SiC grains [7, 8], and introducing long aspect ratio and high strength reinforcements [9–11]. The increase in fracture toughness (7.6 MPa m$^{1/2}$ evaluated by single edge notch beam method) with variation of microstructure is attributed to the enhanced crack deflection and bridging [1–14]. However, the mechanical characteristics of particulates (grains), whiskers, and carbon nanotubes toughened SiC matrix composites need to be much more improved for further applications.

SiC is a highly covalent, bonded compound and, therefore, very difficult to densify. Many attempts have been made to densify SiC matrix composites. These approaches include the conventional solid state sintering using boron and carbon as sintering aids, liquid state sintering using metal oxides as sintering aids and reaction sintering by immersing green preforms into the melted silicon [1–3, 6–9, 15–17]. In addition the innovative in situ synthesis and immersion of green preforms into the Al_2O_3/Y_2O_3 melt have been investigated [4, 5, 10, 11, 18]. Chemical vapor infiltration (CVI) process has been widely used to deposit SiC matrix within the porous fiber preforms to fabricate the fiber reinforced SiC ceramic matrix composites [19–22]. Compared with the above-mentioned approaches, CVI process utilizes low temperature and gas phase route, the as-received aspect ratio, morphology, and mechanical properties of reinforcements can be maintained and the volume fraction of reinforcements can be significantly

---

Y. Hua (✉) · L. Zhang · L. Cheng
National Key Laboratory of Thermostructure Composite Materials, Northwestern Polytechnical University,
Xi'an 710072, People's Republic of China
e-mail: nanojing@163.com

Y. Hua · Z. Li · J. Du
Northwest Institute for Nonferrous Metal Research,
Xi'an 710016, People's Republic of China

high, which can greatly improve the fracture toughness of composite [12–14]. However, few works have been made to densify the particulates and whiskers reinforced SiC matrix composites by CVI.

In this work, CVI is used to deposit SiC matrix in the porous SiC particulate and whisker preforms to prepare particulates and whiskers reinforced SiC ceramic matrix composites (SiC_P/SiC and SiC_W/SiC), respectively. The density, microstructure, and mechanical properties of SiC_P/SiC and SiC_W/SiC were investigated.

Experimental

Composites preparation

The numerical simulation had shown that the fiber preforms consisted of the small pores and the large pores of moderate size can be densified into the composites with the highest density [23]. In this work, the size of β-SiC particulates (98% β-SiC, WEIFANG KAIHUA, Shandong, PR China) is $d_{50} = 5$ µm. The particulates have a faceted shape. β-SiC whiskers (99% pure, Alfa Aesar, MA, USA) has an average size of 18 µm in length and 1.5 µm in diameter and a burl profile.

The particulates and whiskers were acid leached to remove the SiO_2 and metal impurities. The as-treated particulates and whiskers were mixed with the liquid polycarbosilane (PCS, 99.8% pure, Laboratory of Advanced Materials, Xiamen University, Xiamen, PR China) 6% mixed hexane and acetylacetone solution, respectively. Then the solvent was extracted by a rotary evaporator. The particulates and whiskers coated with the PCS were cold pressed to a Ø50 mm × 1.5 mm piece at 40 and 10 MPa, respectively. The green density of particulate and whisker pre-compacts was 68.5 and 47.2%, respectively. Then, the pre-compacts were crushed and screened to select the agglomerates. The diameter of both whisker agglomerates and particulate agglomerates ranges from 200 to 400 µm. The agglomerates were heat treated at 1473 K for 2 h at Ar atmosphere. As-heat treated particulate and whisker agglomerates were cold pressed into the porous preforms with the dimension of Ø40 mm × 3.5 mm, respectively. The particulate or whisker preforms has two types of pores; one is small pores of several micrometers at inter-particulates (or whiskers) and the other one is large pores of hundreds micrometers at inter-agglomerates. The volume fraction of large pores in particulate preforms and whisker preforms is 45.7 and 47.0%, respectively. The green density of particulate and whisker preforms, namely, the volume fraction of SiC particulates and whiskers, was 37.2 and 25.0%, respectively. The schematic diagram of particulate (or whisker) preform structure is shown in Fig. 1.

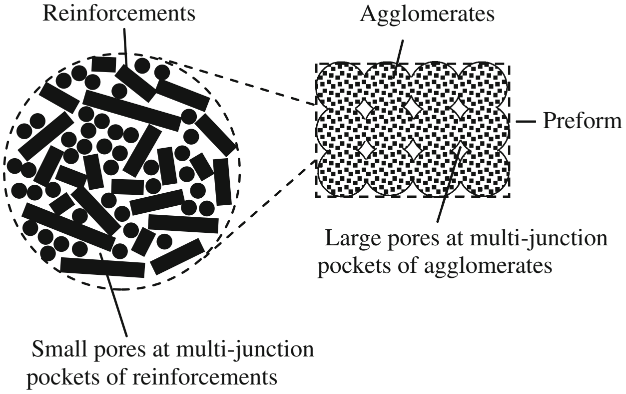

Fig. 1 Schematic diagram of particulate (or whisker) preform structure

Chemical vapor infiltration was performed to deposit SiC matrix in the particulate and whisker preforms for 400 h. Methyltrichlorosilane (MTS: CH_3SiCl_3), hydrogen and argon gas were used as a precursor, a carrier, and dilute gas, respectively. The flow rate of Ar is 350 mL/min, and the input gas ratio of MTS, H_2, and Ar is 1:40:40. The total pressure is 5000 Pa. A deposition temperature was 1273 K. As-received SiC_P/SiC and SiC_W/SiC composites were machined into the specimens with the dimensions $3 \times 4 \times 36$ mm^3 and $2.5 \times 5 \times 24$ mm^3, respectively. Then the SiC_P/SiC and SiC_W/SiC specimens were further deposited SiC matrix for 100 h. The SiC_P/SiC and SiC_W/SiC composites infiltrated SiC for 500 h were used for the following test and analysis.

Characterization and mechanical tests

Bulk density of SiC_P/SiC and SiC_W/SiC composites was measured by the Archimedes method. Microstructure was observed using scanning electron microscopy (SEM, JSM-6700F) and transmission electron microscopy (TEM, JEM 3010) together with electron diffraction. The polished surface was etched with a mixture of molten salts ($NaOH + K_3Fe(CN)_6$) to observe microstructure. A three-point flexure test with a specimen size of $3 \times 4 \times 36$ mm^3 was performed to measure the flexural strength. The span length and the cross-head speed were 30 mm and 0.5 mm/min, respectively. Five specimens were tested at room temperature to obtain an average value. Fracture toughness was measured by the single edge notched beam (SENB) method with a specimen size of $2.5 \times 5 \times 24$ mm^3. The span was 20 mm and the depth and width of the specimen notch was 2.5 mm and less than 0.2 mm, respectively. Five specimens were measured at room temperature to obtain an average value.

Results and discussion

Density analysis

Table 1 shows the density of SiC_P/SiC and SiC_W/SiC composites. The theoretical density of CVI–SiC, SiC particulates and SiC whiskers is considered as 3.19 g/cm^3. The density of SiC_P/SiC and SiC_W/SiC composites is low compared to that of SiC matrix composites prepared by the pressureless sintering (>95% theoretical density) and hot pressing (>98% theoretical density) [9, 16, 17, 24]. Composites prepared by the CVI process intrinsically have the significant residual porosity (typically, about 10–15%) by clogging effects [19–22].

The final density of SiC_P/SiC and SiC_W/SiC composites is higher than that of carbon or silicon carbide fiber reinforced SiC ceramic matrix composites, because both the diameter of particulates (or whiskers) and the diameter of agglomerates are smaller and more suitable to the CVI process than that of fiber filaments and bundles [23]. The relative density of SiC_W/SiC composites is improved from 88.72 to 90.28% after employing whisker agglomerates of moderate size [23, 25]. The final density of SiC_P/SiC composites is higher by 1.88% than that of SiC_W/SiC composites. The particulate preforms is preferable to achieve a higher final density. The microstructure and volume fraction of large pores in particulate preforms is almost same as that in whisker preforms, so the density gain in the multi-junction pockets of particulate agglomerates is the same as that of whisker agglomerates. The green density of particulate preforms is higher by 12.2% than that of whisker preforms. Therefore, the density gain in the whisker agglomerates is much higher than that in particulate agglomerates.

Table 1 The final density of SiC_P/SiC and SiC_W/SiC composites

Composites	Density (g/cm^3)	Relative density (%)
SiC_P/SiC	2.94	92.16
SiC_W/SiC	2.88	90.28

Microstructure and phase studies

The typical microstructure of SiC_P/SiC and SiC_W/SiC composites is shown in Fig. 2. The microstructure of both materials consisted of the particulate (or whisker) reinforced SiC agglomerates, SiC matrix phase located

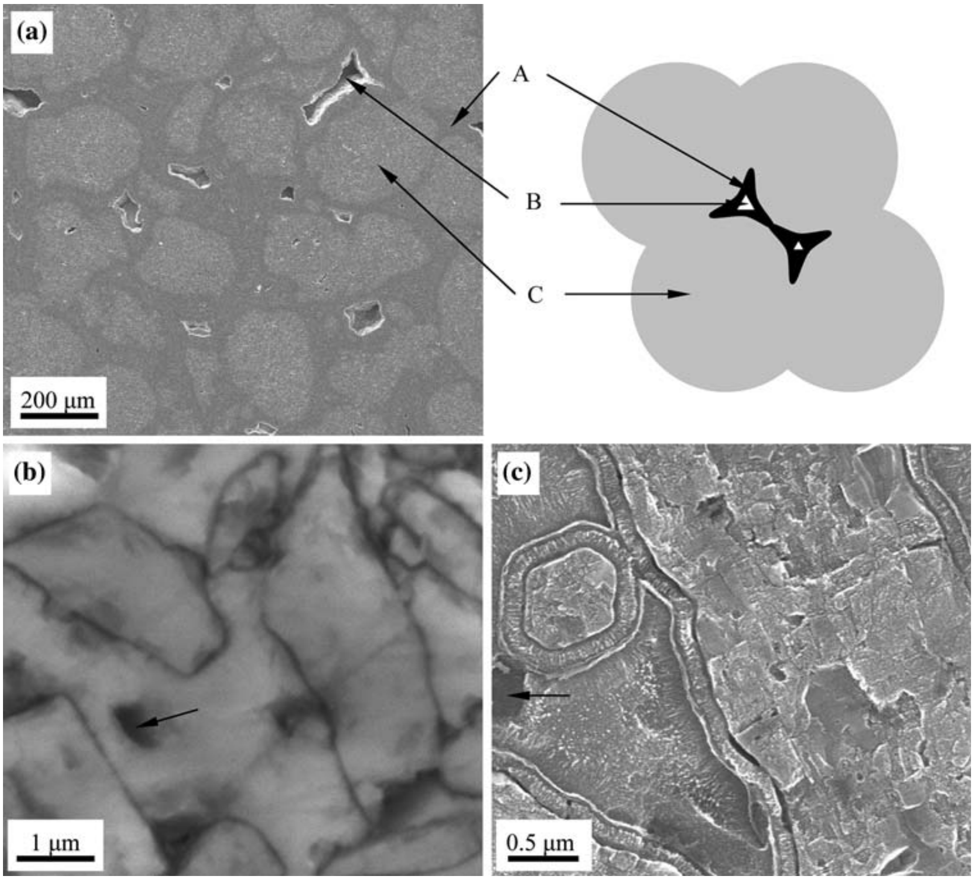

Fig. 2 Typical microstructure and structural schematic diagram of SiC_P/SiC (and SiC_W/SiC) composites. **a** *A*, *B*, and *C* represent the CVI–SiC matrix at the multi-junction pockets, close pores at the multi-junction pockets, and connected SiC_P/SiC (or SiC_W/SiC) composites, respectively. **b** and **c** show the etched surface of connected SiC_P/SiC and SiC_W/SiC composites, respectively. The *arrow* shows the closed pores at the multi-junction pockets of reinforcements

inter-agglomerates and two types of pores located inter-particulates (or whiskers) and inter-agglomerates. Figure 2b and c shows the connected SiC_P/SiC and SiC_W/SiC agglomerates, respectively. It can be seen from Fig. 2b and c that there are a few closed pores (shown by arrow), and the particulates and whiskers retain their original faceted and burl morphology, respectively. This microstructure can be explained by the structural feature of particulate (or whisker) preforms. The small pores in the agglomerates and the large pores among the agglomerates are connected with each other. The densification takes place simultaneously in the small pores and large pores. The infiltration in the small pores terminates earlier due to its significantly high accessible surface area. The close pores at the multi-junction pockets of reinforcements are formed due to the clogging effect of gas transfer [19–22]. And then densification takes place successively in the large pores among agglomerates at the following stages, resulting in the deposition of connected CVI–SiC matrix. The porous preforms are ultimately densified into the composites after the infiltration in the large pores terminates, and the close pores at the multi-junction pockets are formed due to the clogging effect [19–22].

The clogging effect will lead to a density gradient along the bulk composites and the agglomerates. Figure 3 shows the microstructure of SiC_W/SiC composites near the outer surfaces and near the center. It can be seen from Fig. 3 that the density of bulk composites near the outer surfaces is slightly higher than that near the center and the density of agglomerates near the outer surfaces is higher than that near the center.

The crystallization behavior of pyrolyzed PCS dependent on the temperature had been investigated [26]. The PCS heat treated at 1473 K produces crystalline β-SiC of 7 nm grain size and a small amount of carbon [26]. Figure 4 shows the HRTEM image of whisker/matrix interface and

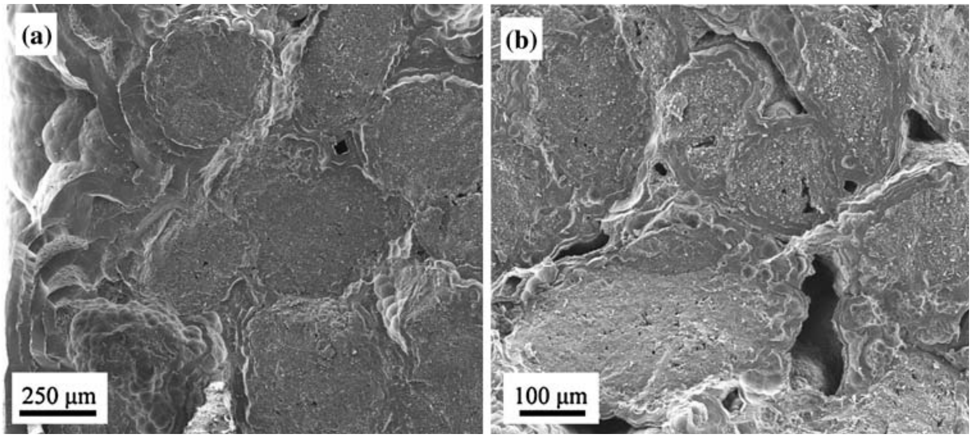

Fig. 3 Typical microstructure of SiC_W/SiC (or SiC_P/SiC) composites **a** near the outer surfaces and **b** near the center

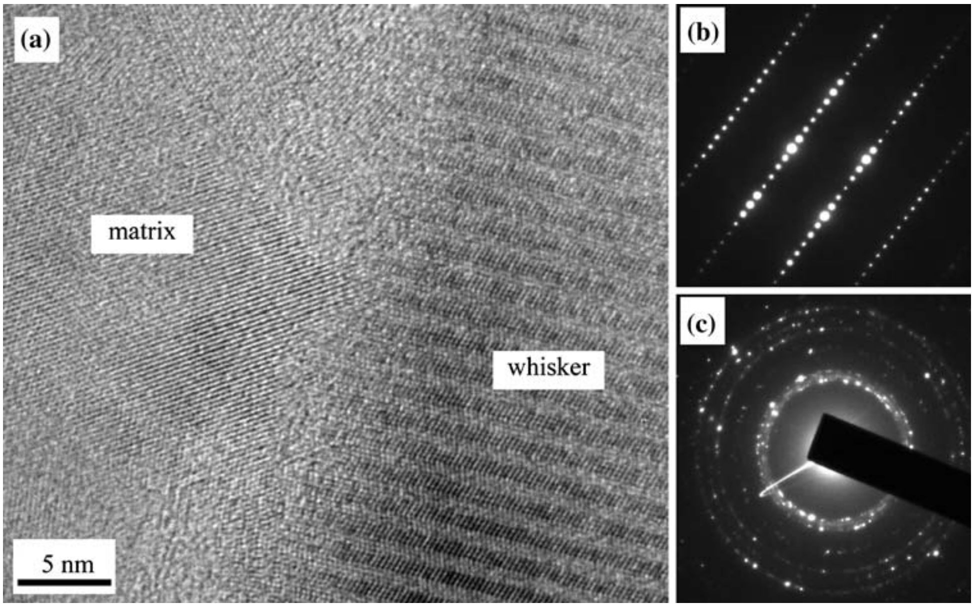

Fig. 4 HRTEM image of whisker/matrix interface (**a**) and electron diffraction pattern of whisker (**b**) and matrix (**c**) in SiC_W/SiC composites

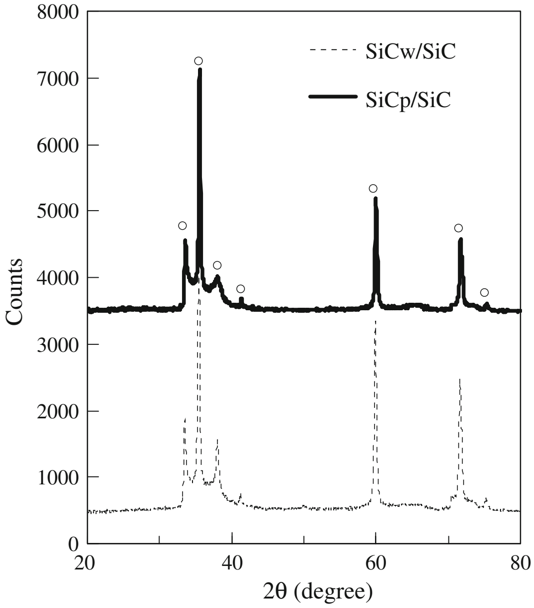

Fig. 5 The XRD patterns of SiC_W/SiC and SiC_P/SiC composites. *Open circle* SiC

electron diffraction pattern of whisker and matrix in SiC_W/SiC composites. Typical whisker/matrix interface observed by HRTEM shows no presence of an inhomogeneous interface phase. As revealed by electron diffraction in Fig. 4c, PCS pyrolysis produces polycrystalline SiC. Figure 5 shows the XRD patterns of SiC_W/SiC and SiC_P/SiC composites, and only SiC phases are detected. Carbon is not detected in this work. The different phases in Fig. 2c are the deposition interfaces in matrix in agglomerates.

Mechanical property studies

The fracture toughness and flexural strength of SiC_P/SiC and SiC_W/SiC composites are reported in Table 2. Both the fracture toughness and flexural strength of SiC_W/SiC composites are higher than that of SiC_P/SiC composites, although the latter composites have higher density and volume fraction of reinforcements. This indicates that SiC whiskers incorporating into the SiC matrix provides better strengthening and toughening effects than SiC particulates does.

The fracture toughness of SiC_W/SiC composites increases with increasing its density due to the decreased pore size and increased flexural strength [8, 25, 27]. The fracture toughness of SiC_W/SiC composites is higher than the best data from other studies, which was 7.6 MPa $m^{1/2}$ for AlN–SiC composites [1–11]. The bonding strength between whiskers and matrix should be strong enough for the whiskers to toughen and strengthen matrix due to its short aspect ratio. Silicon nitride whiskers reinforced homogeneous silicon nitride ceramic matrix composites prepared by hot pressing without sintering aids shows a complete brittle fracture [28]. This is due to the bonding strength between the whiskers and the matrix is too strong when there is no inhomogeneous interface phase between them [8, 28–31]. The aspect ratio of fiber can be considered as infinitely long. The bonding strength between fibers and matrix could be weak enough for the fibers to toughen and strengthen matrix due to its infinitely long aspect ratio. When there is no pyrolysis carbon interface between the fibers and the matrix, the bonding strength between them generated by CVI is too strong, inducing a brittle fracture of fibers reinforced silicon carbide composites. An appropriately strong bonding strength between whiskers and matrix can improve both the fracture toughness and flexural strength of composites [30]. The aspect ratio of whiskers in this work is about 12. There is no inhomogeneous interface phase between whiskers and CVI–SiC matrix but the fracture toughness of SiC_W/SiC composites is significantly improved. It can be concluded that the CVI process would result in a relatively weak bonding strength between the SiC matrix and the homogeneous SiC particulates or whiskers than the sintering process does.

Table 2 Fracture toughness and flexural strength of SiC_P/SiC and SiC_W/SiC composites

Composites	Fracture toughness (MPa $m^{1/2}$)	Flexural strength (MPa)
25.0 vol.% SiC_W/SiC	8.34 ± 0.27	425 ± 32
37.2 vol.% SiC_P/SiC	6.18 ± 0.27	373 ± 25

The flexural fracture surface of SiC_P/SiC and SiC_W/SiC composites is shown in Fig. 6. It appeared to be quite rough with evidence of inter-particulate and transparticulate fracture mode for SiC_P/SiC composites and intergranular and transgranular fracture mode for SiC_W/SiC composites. The burl profile of whiskers can be seen in the fracture surface, which results in a short pullout length. The particulates does not show obvious pullout due to its faceted profile. The crack path generated by indentation is shown in Fig. 7. Crack deflection and bridging are pronounced in both SiC_P/SiC and SiC_W/SiC composites. It can be seen that the crack propagation paths are strongly influenced by the reinforcement morphology and reinforcement orientation to the proceeding crack plane. For the crack plane normal to the reinforcement axis, the reinforcements generally rupture and the cracks propagate across the reinforcements. For the crack plane inclined to the reinforcements, the cracks deflect along the reinforcements/matrix interface, and then the cracks pass over the reinforcements when the reinforcement surface is smooth, or then the reinforcements rupture when the reinforcement surface is rough and causes stress concentration. Compared with the toughening contribution to composites by whisker

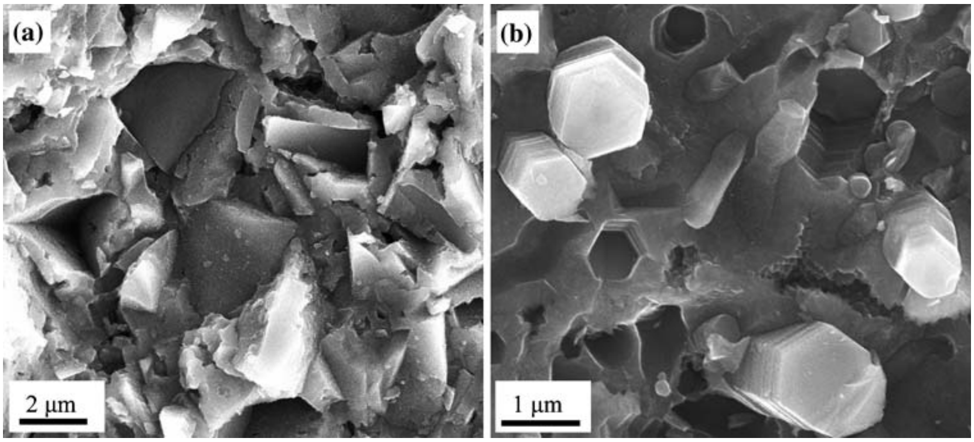

Fig. 6 SEM micrograph of fracture surface of **a** SiC_P/SiC and **b** SiC_W/SiC composites. The jagged surface testifies to higher measured fracture toughness

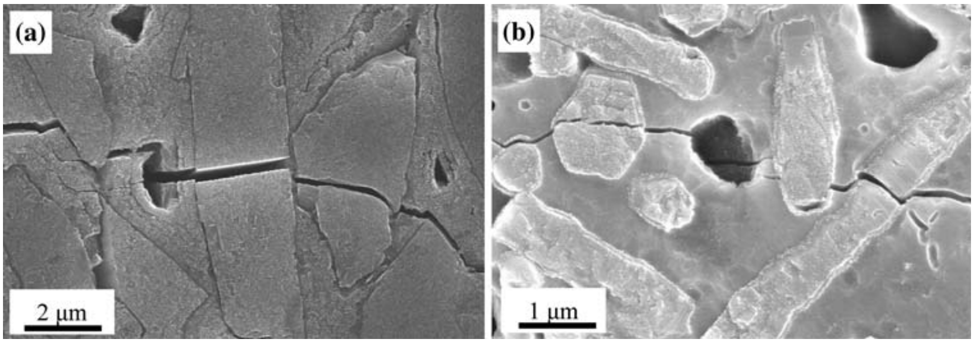

Fig. 7 SEM micrograph of crack paths from Vickers indentation in **a** SiC_P/SiC and **b** SiC_W/SiC composites

bridging, that by particulate bridging is not significant because fracture strength of particulates is much lower than that of whiskers [14]. The main toughening contribution to SiC_P/SiC is crack deflection because the volume fraction of particulates is significantly high and the particulates have a rod-like faceted profile [12]. The main toughening contribution to SiC_W/SiC is crack deflection and bridging because the aspect ratio and fracture strength of whiskers are significantly high.

The flexural strength of particulates and whiskers (including carbon nanotubes) reinforced ceramic matrix composites is limited by the defects, inclusions or grain size, and increases with increasing its density [5, 8, 10, 25, 32, 33]. SiC_P/SiC and SiC_W/SiC composites have a relatively low flexural strength because there exist inevitable closed pores at the multi-junction pockets as shown in Fig. 2 [5, 10, 34]. The relationship of critical aspect ratio (L_C) and fracture strength (σ_{Ru}) of reinforcement with interface shear strength (τ_i) can be described as

$$L_C = \sigma_{Ru}/2\tau_i \qquad (1)$$

where τ_i is equal to the bonding strength between whisker and CVI–SiC matrix. The fracture strength of whisker can be as high as 21 GPa. If the stress can be completely transferred from the matrix to the whisker with critical aspect ratio of 12, the bonding strength between whisker and matrix should be as high as 875 MPa. The whisker with aspect ratio of 12 may not reach the critical aspect ratio at the given bonding strength between whisker and CVI–SiC matrix, so the SiC_W/SiC composites could not be effectively strengthened by the whiskers. In addition, SiC_W/SiC composites is not significantly strengthened by whiskers is partly due to the whiskers that are parallel to the crack plane cannot have much stress transfer from the matrix [35, 36].

Conclusions

SiC_P/SiC and SiC_W/SiC composites were prepared by the CVI process through depositing SiC matrix in the porous particulate and whisker preforms, respectively. The particulate or whisker preforms has two types of pores; one is small pores of several micrometers at inter-particulates (or whiskers) and the other one is large pores of hundreds micrometers at inter-agglomerates. SiC_P/SiC (or SiC_W/SiC) consisted of the particulate (or whisker) reinforced SiC agglomerates, SiC matrix phase located inter-agglomerates and two types of pores located inter-particulates (or whiskers) and inter-agglomerates. The high volume fraction of rod-like faceted particulates and the relatively weak interface bonding strength between particulates and matrix result in the improved fracture toughness of SiC$_P$/SiC, which is as high as 6.18 MPa m$^{1/2}$, mainly owing to crack deflection. The high fracture strength and long aspect ratio of whiskers and the relatively weak interface bonding strength between whiskers and matrix result in the improved fracture toughness of SiC$_W$/SiC, which is as high as 8.34 MPa m$^{1/2}$, mainly owing to crack deflection and bridging. The relative density of SiC$_P$/SiC and SiC$_W$/SiC composites was 92.16 and 90.28%, respectively. The flexural strength of SiC$_P$/SiC and SiC$_W$/SiC composites was 373 and 425 MPa, respectively. The relatively low flexural strength of SiC$_P$/SiC composites is mainly due to its low density. The relatively low flexural strength of SiC$_W$/SiC is mainly due to its low density, relatively low bonding strength between whisker and matrix and the randomly oriented whiskers that are parallel to the crack plane cannot have much stress transfer from the matrix. SiC whiskers incorporated into the SiC matrix provides better strengthening and toughening effects than SiC particulates does.

Acknowledgements The authors acknowledge the support of this work by the Natural Science Foundation of China under Grant No. 90405015.

References

1. Lee SK, Kim DY (2002) J Mater Sci Lett 21:1343
2. Kim YW, Kim JY, Rhee SH, Kim DY (2000) J Eur Ceram Soc 20:945
3. Cho KS, Choi HJ, Lee JG, Kim YW (1998) Ceram Int 24:299
4. Padure P (1994) J Am Ceram Soc 77(2):519
5. Tani T (1999) Composites Part A 30:419
6. Strecker K, Hoffmann MJ (2005) J Eur Ceram Soc 25:801
7. Dong SM, Jiang DL, Tan SH, Guo JK (1995) Ceram Int 21:451
8. Pan YB, Qiu JH, Kawagoe M, Morita M, Tan SH, Jiang DL (1999) J Eur Ceram Soc 19:1789
9. Mahfuz H, Zadoo DP, Wilks F, Maniruzzaman Md, Jeelani S (1995) J Mater Sci 30:2406. doi:10.1007/BF01184593
10. Hirota K, Hara H, Kato M (2007) Mater Sci Eng A 458:216
11. Morisada Y, Miyamoto Y, Takaura Y, Hirota K, Tamari N (2007) Int J Refract Met Hard Mater 25:322
12. Faber KT, Evens AG (1983) Acta Metall 31(4):565
13. Faber KT, Evens AG (1983) Acta Metall 31(4):577
14. Becher PF, Hsueh CH, Angelini P, Tiegs TN (1988) J Am Ceram Soc 71(12):1050
15. Paik U, Park HC, Choi SC, Ha CG, Kim JW, Jung YG (2002) Mater Sci Eng A 34:267
16. Magnani G, Beltrami G, Minoccari GL, Pilotti LJ (2001) J Eur Ceram Soc 21(5):633
17. Lillo TM, Bailey DW, Laughton DA, Chu HS, Harrison WM (2003) Ceram Eng Sci Proc 24(3):359
18. Taguchi SP, Ribeiro S, Balestra RM, Rodrigues D Jr (2007) Mater Sci Eng A 454–455:24
19. Naslain R (2004) Compos Sci Technol 64(2):155
20. Besmann TM, Lowden RA, Stinton DP (1993) In: Naslain R, Lamon J, Doumeingts D (eds) High temperature ceramic matrix composites. Woodhead Publishing Ltd, Cambridge, p 215
21. Lackey J, Hanigofsky JA, Freeman GB, Hardin RD, Prasad A (1995) J Am Ceram Soc 78(6):1564
22. Xu YD, Zhang LT (1997) J Am Ceram Soc 80(6):1897
23. Hua YF, Zhang LT, Cheng LF, Li ZX, Du JH (2009) Comput Mater Sci 46:133
24. She JH, Jiang DL, Tan SH, Guo JK (1995) Key Eng Mater 108–110:45
25. Hua YF, Zhang LT, Cheng LF, Wang J (2006) Mater Sci Eng A 428:346
26. Li HB, Zhang LT, Cheng LF, Wang YG, Yu ZY, Huang MH, Tu HB, Xia HP (2008) J Mater Sci 43:2806. doi:10.1007/s10853-008-2539-8
27. Kodama H, Miyoshi T (1992) J Am Ceram Soc 75(6):1558
28. Tanaka I, Pezzotti G, Miyamoto Y, Okamoto T (1991) J Mater Sci 26:208. doi:10.1007/BF00576053
29. Ueno K, Kose S, Kinoshita M (1993) J Mater Sci 28:5770. doi:10.1007/BF00365180
30. Yanai T, Ishizaki K (1996) Mater Trans JIM 37(12):1802
31. Kim YW (2001) J Am Ceram Soc 84(9):2060
32. Zhu SM, Fahrenholtz WG, Hilmas GE (2007) J Eur Ceram Soc 27:2077
33. Baldacim SA, Santos C, Silva OMM, Silva CRM (2003) Int J Refract Metals Hard Mater 21:233
34. Dong SM, Jiang DL, Tan SH, Guo JK (1999) J Inorg Mater 14(1):61
35. Baldacim SA, Cairo CAA, Silva CRM (2001) J Mater Process Technol 119:273
36. Goto Y, Tsuge A (1993) J Am Ceram Soc 76(6):1420